

PAPER • OPEN ACCESS

Control of the metal crystallization process by the modulated traveling magnetic field

To cite this article: G L Losev *et al* 2018 *J. Phys.: Conf. Ser.* **1128** 012051

View the [article online](#) for updates and enhancements.

You may also like

- [Metal complex catalysis in the synthesis of organoaluminium compounds](#)
Usein M Dzhemilev and Askhat G Ibragimov
- [Photons and leptons in external fields at finite temperature and density](#)
A V Borisov, A S Vshivtsev, V Ch Zhukovskii et al.
- [Comment on 'Matrix generalization of the modified Korteweg-de Vries equation'](#)
Qing Ping Liu and C Athorne



ECS
The
Electrochemical
Society
Advancing solid state &
electrochemical science & technology

DISCOVER
how sustainability
intersects with
electrochemistry & solid
state science research

Control of the metal crystallization process by the modulated traveling magnetic field

G L Losev, I V Kolesnichenko, R I Khalilov

Institute of Continuous Media Mechanics Ural Branch Russian Academy of Sciences,
614013, Academician Korolev Street 1, Perm, Russian Federation

E-mail: losev.g@icmm.ru, kiv@icmm.ru, khalilov@icmm.ru

Abstract. The influence of a modulated traveling magnetic field on the process of crystallization of a liquid conducting medium is experimentally investigated. The crystallization process is carried out in a vertical cell with a constant temperature difference between the narrow walls of the layer. A traveling magnetic field produced by a linear inductor generates a vortex flow in the medium. This flow leads to redistribution of temperature and change in the position of the crystallization front. Low-frequency modulation of the traveling field leads to generation of significantly pulsating flow. This has a positive effect on the stirring efficiency of the medium. In addition, the flow smoothes the crystallization front, reducing the speed of its movement.

1. Introduction

Production of alloys with special properties is one of the priority areas of metallurgy these days. Stirring of metals during the crystallization process leads to an increase in the mechanical strength of ingots, homogenization of distribution of impurity inclusions, and grinding of the grain of metal [1–3]. In practice, the method has been used for contactless mixing of metal by application of traveling or rotating magnetic fields in closed volumes [4] or during metal transportation through technological channels [5]. Contactless generation of the molten metal flow is useful for continuous casting. Besides, the application of stirrers for manufacturing cylindrical ingots in aluminum semicontinuous casting machines is being extensively investigated (e.g., [6]).

An alternating magnetic field creates eddy currents in a conducting medium. The interaction of these currents with the initial magnetic field leads to generation of an electromagnetic force and, as a consequence, vortex flows in liquid metals. The flows increase the efficiency of heat transfer in the melt and smooth the crystallization front [7, 8]. Modulation of the magnetic field allows reduction of the energy costs in the process of metal processing, and also potential increase in effectiveness of mixing.

The experimental study of processes in the electromagnetic stirrers is connected with a number of difficulties due to high melting point and chemical activity of most metal alloys. The existing optical methods (e.g. PIV) cannot be used for this purpose because of the optical opacity of liquid metals. Due to the practical difficulty of studying processes in the real fabrication systems, there is a need for laboratory modeling of the investigated devices (including the use of low-melting alloys). For this reason, application of an Ultrasound Doppler velocimeter (UDV) is justified. This device has been widely used in similar researches (e.g., [9–12]).



This work is devoted to modeling the process of liquid metal crystallization under the influence of non-contact electromagnetic stirring. The main purpose of the work is to control the motion of the crystallization front by applying a modulated traveling magnetic field (TMF) to the metal. Geometry of the cavity is consistent with the geometry of cast producing by continuous casting machine. Thus, the obtained results can be used to improve the quality of the metallurgical industry. The results of the work can be also used to verify numerical calculations.

2. Methods

An experimental setup (figure 1) consists of vertical cell 1, made of plexiglass. The cell is filled with liquid alloy GaSnZn (melting point is 18°C). The cell is 450 mm long, 20 mm width and 75 mm height.. Two copper heat exchangers 2 are placed at the thin walls of the cell. Vertical sides of the cell are thermally insulated by layers of glass wool. The upper boundary of the metal is free and has heat exchange with the ambient. The temperature control is carried out by means of two thermostats 3 CRIO-VT-01 with the precision of $\pm 0.5^\circ\text{C}$. The temperature of “hot” heat exchanger is 20°C and the temperature of the “cold” one is -30°C . After the crystallization process starts the temperatures of the heat exchangers are steady during all the time of the experiment. The channel is placed on a linear inductor of the TMF 4 with dimensions of $480 \times 350 \text{ mm}^2$. The TMF is created by six coils (170 turns in one coil). The coils are powered by a three-phase programmable current source 5 Pacific Smart Source 360 ASX-UPC3. This power supply allows one to specify the shape of the output signal and modulate the TMF. The frequency of supplied current is 50 Hz. The measurements of the crystallization front position and velocity of the flows in liquid metal phase are made by means of ultrasonic Doppler velocimeter 6 (UDV) DOP 2000, Signal Processing. Four sensors 7 of the UDV is placed on the thin wall of the cell. The ultrasonic rays pass through the ports in the “hot” heat exchanger. Ultrasound Doppler velocimetry includes emitting ultrasound wave packages by an ultrasonic sensor, their consequent adoption, and calculation of the Doppler frequency shift between the emitted and received wave packages. The ultrasonic silicone gel has to be used to provide sound contact between the probe and the wall. However, the presence of sound-reflecting particles moved by the flow in the medium is necessary. The gallium oxide particles reflect ultrasound waves in gallium eutectic. These particles are formed by oxidation of gallium in the atmosphere [13]. A significant part of the ultrasonic wave energy is reflected on the solid/liquid interface. This leads to forming of the peak in the echo-signal. The peak position on the coordinate axis corresponds to the position of the crystallization front. So the solid/liquid interface position can be measured by the UDV [11, 14].

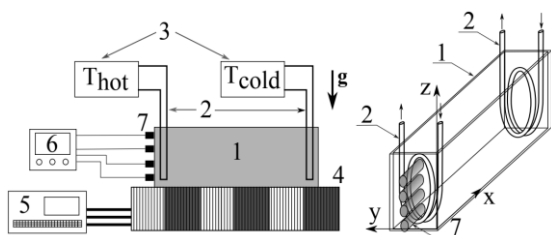


Figure 1. Sketch of the experimental setup: 1. channel filled with liquid metal, 2. heat exchangers, 3. thermostats, 4. linear induction machine, 5. power supply, 6. UDV, 7. ultrasonic sensors.

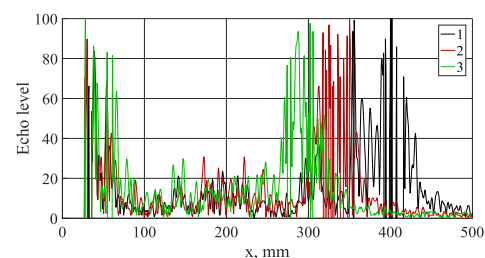


Figure 2. Examples of the echo-signals in different moments of time: 1. – 3.5 s, 2. – 3050 s, 3. – 6120 s.

Figure 2 demonstrates examples of the echo-signals in different moments of time. To find the position of the peak on the spatio-temporal distribution of the echo signal, the wavelet analysis was used. The found dependencies of the crystallization front positions on time are approximated by linear

functions. The averaged velocity V of the crystallization front movement is calculated by differentiating the approximated lines.

3. Results

The dependence of crystallization front positions on time for three values of TMF is shown in figure 3. As the crystallization front shifts, the region covered by the stirring flow decreases. Due to this, the heat exchange rate decreases with time, which leads to a decrease in the velocity of the solid/liquid interface movement.

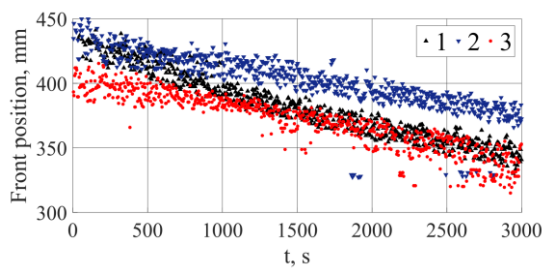


Figure 3. The change of the crystallization front position vs time at the power supplies: 1. – 0 A, 2. – 3.0 A, 3. – 5.0 A.

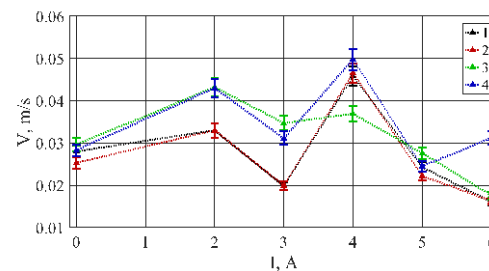


Figure 4. The dependence of the crystallization front movement velocity on the supply current at different altitudes: 1. – 19 mm, 2. – 35 mm, 3. – 51 mm, 4. – 67 mm.

Nonlinearity of dependence of the crystallization front movement velocity on the value of the TMF can be due to a qualitative conversion of the flow that appears in the liquid phase. A large-scale flow of high intensity results in washing away of the "cold" liquid into the bottom region. In the remaining part of the layer, the reverse flow heats the metal. As a result, continuous heat transfer to the crystallization region is formed, which significantly reduces the rate of crystallization. Low-intensity flows provide insufficiently effective stirring, although they smooth out the crystallization front. This results in a slight increase in the velocity of the crystallization front movement.

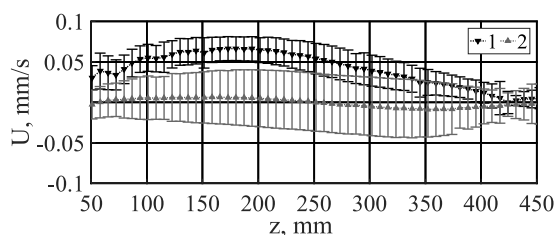


Figure 5. Spatio profiles of flow velocity (supply current 4.0 A, main current frequency 50 Hz): 1. no modulation, 2. modulation period 50 s.

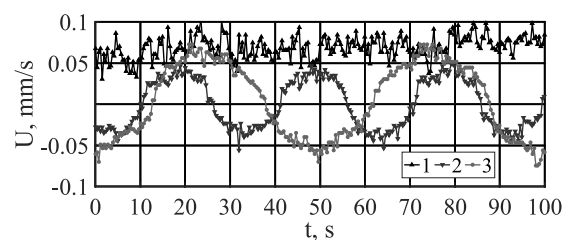


Figure 6. Flow velocity evolutions at few periods of modulation: 1. no modulation, 2. modulation period 30 s, 3. modulation period 50 s.

To further improve the efficiency of metal stirring and temperature equalization in the entire volume of the cell, the TMF was modulated with frequencies 0.02 – 0.1 Hz. The TMF was created by the current 4.0 A with a maximum of the crystallization front movement velocity. Over the period, the magnitude of the magnetic induction changed its value according to the sinusoidal law. In the second half-cycle, a change in the direction of the TMF occurred. This reverse modulation generates a pulsed flow in the liquid phase. Figure 7 demonstrates spatial-temporal distribution of the metal flow velocity U . The vertical bands on the map represent variation of the velocity U generated by the modulations of

TMF. This flow is significantly oscillatory. This leads to the increase in heat exchange and, consequently, alignment of the crystallization front along the entire height of the cell.

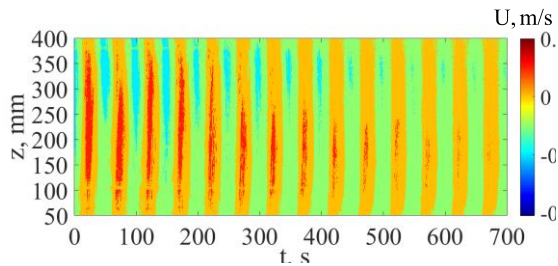


Figure 7. Spatial-temporal distribution of the liquid metal flow velocity in the height of 35 mm.

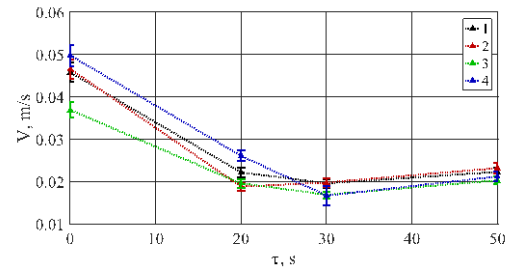


Figure 8. The crystallization front movement velocity vs period of reverse modulation measured by four UDV transducers.

Low-frequency modulations change the structure of the flow generated in the liquid metal. The large-scale averaged vortex decays when the reversal modulations are applied. It becomes replaced by a pulsating (around zero mean velocity) flow (figure 5–7). The amplitude of the velocity pulsations of the flow caused by the modulated TMF is almost half as much as the pulsation, and the average component of the flow velocity generated by the non-modulated TMF. The TMF modulation period determines directly the frequency of oscillations of the generated flow. In this case, the amplitude of pulsations is slightly changed.

The dependencies of crystallization front movement velocity measured by four UDV probes on the period of modulations of the TMF are shown in figure 8. It is seen that the crystallization front movement velocities at different heights of the cell are close. The velocity of the solid/liquid interface motion depends little on the modulation period, provided its value differs from zero.

4. Conclusion

Imposition of the TMF on the metal layer during crystallization process leads to stirring of the liquid phase and redistribution of temperature along the cell. The velocity of the crystallization front movement depends on the magnitude of the TMF non-monotonically. The high-intensity flow generated by electromagnetic force leads to washing away of the cooled metal into the bottom region of the cell. In this case, the crystallization front moves predominantly in the vertical direction. The low-intensity flows equalize the temperature of the metal in the central part of the channel. In this region, the metal is in the solid/liquid state (there are inclusions of the crystallized metal in the liquid phase). The liquid and solid phases occupy only small regions (of the order of 1.5–2 cm) near the heat exchangers. The highest velocity of the crystallization front motion is observed at the supplied current of 4.0 A. In this case, the crystallization of metal occurs uniformly in the entire region except for a thin layer in the central part of the cell.

Low-frequency reversal modulation of the TMF lowers the rate of crystallization, but smooths the crystallization front due to the increase in the stirring efficiency of the different-temperature layers of the liquid metal. The crystallization front moves with close velocities along the entire height of the layer at all studied modulation frequencies. At the same time, the velocity of the solid/liquid interface movement depends weakly on the modulation frequency.

Thus, electromagnetic stirring regimes providing the maximum velocity of the crystallization front movement have been found there. The considered modes of the TMF modulation provide an effective alignment of the phase interface.

Acknowledgments

This work was supported by the RFBR grant 17-48-590539_r_a.

References

- [1] Willers B, Eckert S and Nikrityuk P A 2008 *Metall. Mater. Trans.* **39** 304–16
- [2] Scepanskis M, Jakovics A and Nacke B 2010 *Magnetohydrodynamics* **46** 413–23
- [3] Denisov S, Dolgikh V and Khripchenko S 2014 *Magnetohydrodynamics* **4** 249–65
- [4] Moffatt H K 1991 *Phys. Fluids A*. **3** 1336–43
- [5] Lielpeter Y 1969 *Liquid metal induction MHD machines* (Riga: Zinatne) 246 (in Russian)
- [6] Mapelli C, Gruttadauria A and Peroni M 2010 *J. Mater. Process. Technol.* **210** 306–14
- [7] Hachani L, Zaidat K and Fautrelle Y 2015 *Int. J. of Heat and Mass Transfer* **85** 438–54
- [8] Avnaim M H, Mikhailovich B, Azulay A and Levy A 2018 *Int. J. of Heat and Fluid Flow* **69** 23–32
- [9] Andreev O, Kolesnikov Y and Thess A 2009 *Exp. Fluids* **46** 77–83
- [10] Ben-David O, Levy A, Mikhailovich B and Azulay A 2013 *Int. J. of Heat and Mass Transfer* **67** 260–71
- [11] Kolesnichenko I, Pavlinov A and Khalilov R 2013 *Magnetohydrodynamics* **49** 191–7
- [12] Franke S, Rabiger D and Galindo V 2016 *Flow Meas. Instrum.* **48** 64–73
- [13] Nowak M 2002 *Exp. In fluids* **31** 249–55
- [14] Oborin P and Kolesnichenko I 2013 *Magnetohydrodynamics* **49** 231–36